Available online at www.sciencedirect.com
ScienceDirect
Journal of Nuclear Materials 363–365 (2007) 775–780
journal of nuclear materials
www.elsevier.com/locate/jnucmat

Helium ash removal by moving-surface plasma-facing components

Y. Hirooka [a,*], S. Hosaka [b], M. Nishiura [a], Y. Ohtsuka [b], M. Nishikawa [b]

[a] National Institute for Fusion Science, 322-6 Oroshi, Toki, Gifu, Japan
[b] Osaka University, 2-1 Yamadaoka, Suita, Osaka, Japan

Abstract

The use of moving-surface plasma-facing components (MS-PFCs) is proposed for the removal of helium ash as well as unburned hydrogenic fuel particles from steady state DT-fusion reactors. A series of proof-of-principle experiments have been conducted, using the VEHICLE-1 facility in which a rotating drum, the simplest form of MS-PFC, can be bombarded with steady state hydrogen, helium and their mixture plasmas with the densities of the order of 10^{10} cm^{-3} and the electron temperatures of 4–5 eV. It has been found from H_α and He–I spectroscopic measurements that the steady state particle removal rates are $\sim 2.5 \times 10^{16}$ H-atoms s^{-1} cm^{-2} and $\sim 1.6 \times 10^{14}$ He-atoms s^{-1} cm^{-2} when the rotating drum is gettered with lithium at the deposition rates of $\sim 2 \times 10^{16}$ Li-atoms s^{-1} cm^{-2} and negative bias voltages of -30 V and -100 V. These data correspond to the average atomic ratios of H/Li $\sim$ 1.25 and He/Li $\sim$ 0.008 in the resultant codeposits. It follows from these findings that hydrogen and helium are not mutually exclusive in the simultaneous codeposition processes, presumably because of their respective preferred trapping sites in lithium deposits.

PACS: 52.40.Hf; 28.52.Fa; 28.52.Lf

Keywords: Helium ash; Lithium gettering; Particle control; Wall recycling

1. Introduction

Ever since the discovery of the 'Supershot' confinement regime in TFTR in late 1980s [1], it has widely been recognized in the magnetic fusion energy research community that high-performance core plasmas often favor reduced wall recycling. To reduce particle recycling, wall conditioning techniques such as boronization have been applied to many plasma confinement experiments. Unfortunately, due to the surface saturation with trapped particles, the efficacy of wall conditioning has a finite lifetime, which necessitates the shutdown of plasma operation for re-conditioning. Clearly, this is not acceptable from the point of view of operating steady state fusion power reactors. It follows from these arguments that enabling wall concepts R&D is necessary for the successful operation of steady state fusion devices beyond ITER (for the International Thermonuclear Experimental Reactor).

* Corresponding author. Tel.: +81 572 58 2628.
E-mail address: hirooka.yoshihiko@nifs.ac.jp (Y. Hirooka).

0022-3115/$ - see front matter © 2007 Elsevier B.V. All rights reserved.
doi:10.1016/j.jnucmat.2007.01.077

Over the past decade, therefore, a variety of innovative plasma-facing component concepts have been proposed to provide a possible resolution for this steady state particle control issue. Essentially all of these concepts employ moving-surface components, either made of a solid or liquid material, for in-line regeneration of particle trapping capabilities. One such concept proposed by Hirooka et al. [2] features a moving-belt made of SiC–SiC fiber fabrics with an in-line getter film deposition system. In our previous work [3–5], proof-of-principle experiments were conducted on this concept with the moving-belt simplified by a titanium- or lithium-gettered rotating drum built in a laboratory-scale linear plasma facility. Results indicate that hydrogen recycling can be reduced to levels significantly lower than 100%, even at steady state, so long as gettering continues.

For the steady state operation of DT-fusion power reactors, not only unburned fuel but helium ash must be removed continuously so as to sustain the nuclear reaction. This means that a substantial pumping speed is necessary for helium ash removal. Given the edge helium partial pressure of the order of 10^{-3} Pa, for example, the power output of 1 GW would require a pumping speed as large as 10^3 m^3/s. Although usually cryogenic pumps are employed for hydrogenic fuel particle control in existing large fusion devices, helium cannot be pumped at the same efficiency due to its extremely low boiling point of 4.2 K. Unfortunately, the use of turbomolecular pumps for helium ash removal is not quite realistic because of the conductance loss along the pumping ducts penetrating thick cryostat walls for superconducting magnets, essential for steady state fusion reactors. Nonetheless, helium ash removal has yet to be addressed as a critical issue in the magnetic fusion community.

In the present work, the use of moving-surface plasma-facing components (to be referred to as MS-PFC in the remainder of this paper) is proposed for the continuous removal of helium ash as well as hydrogenic particles to maintain reduced recycling. It is of particular importance to investigate whether or not helium and hydrogen can simultaneously be incorporated in lithium deposits. Therefore, under hydrogen and helium mixture plasma bombardment, particle recycling from lithium-gettered surfaces has been observed with H_α and He–I spectroscopy, using the same rotating drum setup as described above.

2. Experimental

A linearly magnetized steady state plasma facility: VEHICLE-1 has been used in the present work and the details of this facility have already been presented in our previous paper [6]. In the present work, the ECR power for plasma generation is typically 300 W at which the plasma density is of the order of 10^{10} cm^{-3} and the electron temperature is 4–5 eV. Under these conditions, the total bombarding flux of hydrogenic species is of the orders of 10^{16} H-atoms s^{-1} cm^{-2}, taking into account the contributions from H^0, H^+, H_2^+ and H_3^+.

The main vacuum chamber of VEHICLE-1 is installed with a water-cooled and copper-made rotating drum, the simplest form of MS-PFC, shown in Fig. 1(a). The rotational speed is set at approximately 10 cm/s at the periphery. Evaporated lithium is guided to the drum surface for deposition through a water-cooled stainless steel tunnel, the opening diameter of which is 3.5 cm. The gap between the drum periphery and open end of the vapor-guiding tunnel is only a few mm, so that very little lithium can directly be deposited on the vacuum chamber wall. Note that the rotating drum is maintained at room temperature even under plasma bombardment and lithium gettering.

Shown in Fig. 1(b) is a standing sample tray made of molybdenum on a resistive heater that can be used when post-exposure thermal desorption spectrometry (TDS) measurements are necessary. This tray accommodates a bulk lithium sample in the form of circular disk with the diameter of 2.8 cm and the thickness of 2 mm. Both the rotating drum and sample tray are held independently at the floating potential, so that DC bias voltages can be applied to these 'targets' to be bombarded with plasmas.

Plasma-target interactions in VEHICLE-1 can be diagnosed real-time by a linearly moveable Langmuir probe, optical multi-channel analyzer (OMA), total pressure gauge, residual gas analyzer (RGA), IR pyrometer, and two thermocouples. The plasma column diameter is ~3.5 cm limited by a donut limiter (see Fig. 1(a)) so that the electron density and temperature profiles, measured by the Langmuir probe, are rather uniform over the areas of lithium deposits and the sample tray. For recycling measurements, the OMA is set for H_α and He–I, the volume-integrated intensities of which are measured in front of the rotating drum. Typically, the neutral pressure is ~0.133 Pa (=10^{-3} Torr) during plasma

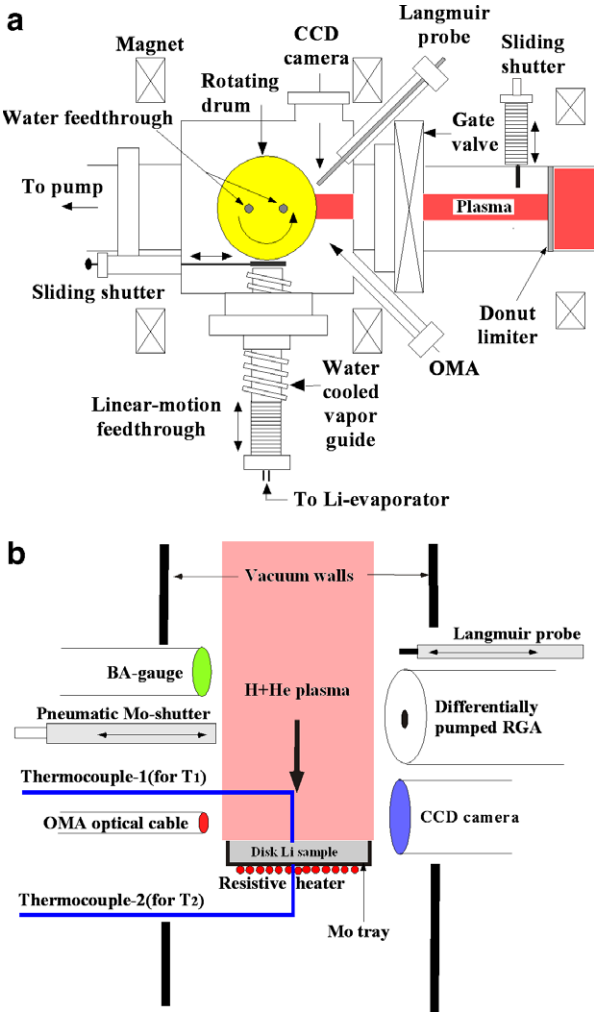

Fig. 1. (a) A schematic diagram of the rotating drum setup in the VEHICLE-1 facility [2] and (b) the standing sample tray setup and PSI-TDS related diagnostics.

operation. To avoid burning the filament, the RGA is housed in a differentially pumped vacuum chamber separated from the main chamber by an orifice creating a pressure ratio of about 100-to-1.

3. Results and discussion

3.1. A brief review of previous work on reduced recycling of helium

In our recent particle recycling experiments [7], it has been demonstrated that helium can be codeposited with lithium on the rotating drum surface during plasma exposure. For these experiments, the lithium deposition rate was $\sim 2\times 10^{16}$ Li-atoms $cm^{-2}\,s^{-1}$, i.e. ~43 Å/s, and the DC bias on the rotating drum was set at −30 V. Spectroscopy data indicated that the He–I intensity decreases by ~20% relative to that without lithium deposition. As opposed to hydrogen, forming lithium hydride with the ionic crystalline structure (see Fig. 2(a)), helium is considered to be trapped in a three-dimensional electrostatic potential 'cage' created at a defect site such as vacancy (see Fig. 2(b)). Note that trapping (or de-trapping) energies of helium by (from) lattice imperfections in metals have been reported to be of the order of a few eV [8], significantly larger than the chemical bonding energy of 0.95 eV for lithium hydride [9]. As it has turned out in more recent experiments, applying a negative DC bias of around a few tens of volts appears to be a 'pre-requisite' to overcome this electrostatic potential barrier.

3.2. Hydrogen and helium mixture plasma exposure and post-exposure TDS

3.2.1. Generation and first-order characterization of mixture plasmas

Hydrogen and helium mixture plasmas are generated with their partial pressures in the main chamber set equal to each other, adjusting the partial pressures measured by the RGA in a differentially pumped chamber such that:

$$P_{\mathrm{He}}^{\mathrm{RGA}}/P_{\mathrm{H_2}}^{\mathrm{RGA}} = \sqrt{m_{\mathrm{H_2}}/m_{\mathrm{He}}} \quad (\because P_{\mathrm{He}} = P_{\mathrm{H_2}}), \tag{1}$$

where $P_{\mathrm{He}}^{\mathrm{RGA}}$ and $P_{\mathrm{H_2}}^{\mathrm{RGA}}$ are the partial pressures in the RGA chamber, P_{He} and $P_{\mathrm{H_2}}$ are the partial

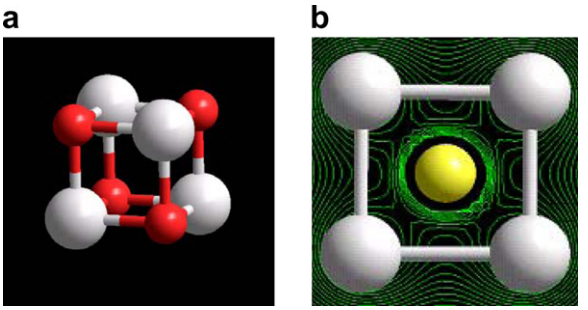

Fig. 2. (a) Chemically bound hydrogen (red) to lithium (white) in the ionic crystal of lithium hydride, and (b) a two-dimensional slice of electrostatic potential contours around helium (yellow) trapped in a vacancy created at the body-centered site of the cubic lattice of solid lithium. The contours are drawn with the increment of 0.01 e/a_{B}, where e is the single electron charge and a_{B} is the Bohr radius.

pressures in the main chamber, and m_{He} and m_{H_2} are the molecular masses of helium and hydrogen, respectively. For the mixture plasma generation, the total pressure is set at ~0.133 Pa ($=10^{-3}$ Torr). It has been found that the electron temperature and density in the mixture plasmas are not significantly different from those measured for individual plasmas.

As to the characterization of hydrogen and helium mixture plasmas, to the best of our knowledge, there are no literature data that can provide relevant information on the species composition for hydrogen and helium mixture plasmas. For simplicity, the formation of compounds such as helium hydride is not taken into account in the afore-mentioned analysis. Available for hydrogen plasmas with parameters identical to those in VEHICLE-1 is the theoretical prediction that ion species: H^+, H_2^+ and H_3^+ will be formed in the following density ratio [10]:

$$n_{H^+} : n_{H_2^+} : n_{H_3^+} \approx 0.1 : 0.3 : 0.6 \tag{2}$$

These individual densities, added to the one for helium ions, can be related to the total plasma density (i.e. electron density), n_e, measured by the Langmuir probe in such a way that:

$$n_{H^+} + n_{H_2^+} + n_{H_3^+} + n_{He^+} = n_e \tag{3}$$

Because the direct formation of H_2^+ from H_2 is the dominant process at electron temperatures 4–5 eV [11,12], for convenience, we approximate the density ratio of $n_{H_2}^+$ to n_{He}^+ in the following manner:

$$\frac{n_{He^+}}{n_{H_2^+}} \approx \frac{n_e n_{He} \langle \sigma v \rangle_{He \to He^+}}{n_e n_{H_2} \langle \sigma v \rangle_{H_2 \to H_2^+}} = \frac{\langle \sigma v \rangle_{He \to He^+}}{\langle \sigma v \rangle_{H_2 \to H_2^+}} \tag{4}$$

where $\langle \sigma v \rangle_{He \to He^+}$ and $\langle \sigma v \rangle_{H_2 \to H_2^+}$ are the electron-impact ionization rate coefficients for the processes: $He \to He^+$ and $H_2 \to H_2^+$, respectively. Note that because the hydrogen and helium partial pressures are set equal for mixture plasma generation, n_{H_2} and n_{He} are cancelled by each other in Eq. (4). Using the atomic and molecular reactions database [12], the ratio $(n_{H_2}^+/n_{He}^+)$ has been calculated to be ~0.1 at $T_e = 4$–5 eV.

Solving Eqs. (2)–(4) with $n_e \simeq 5 \times 10^{10}$ cm^{-3}, the individual species densities have been determined to be: $n_{H^+} \simeq 5 \times 10^9$ cm^{-3}, $n_{H_2^+} \simeq 1.5 \times 10^{10}$ cm^{-3}, $n_{H_3^+} \simeq 2.9 \times 10^{10}$ cm^{-3}, and $n_{He} \simeq 1.5 \times 10^9$ cm^{-3}. Though it is not complete yet, experimental verification on the species composition analysis is under way, connecting the ECR plasma source with a separation magnet.

The total flux of hydrogenic species, including H^0, may be expressed in the following manner [13]:

$$\Gamma_{total} = \Gamma_{H^0} + \Gamma_{H^+} + 2\Gamma_{H_2^+} + 3\Gamma_{H_3^+} \simeq \Gamma_{H^0} + \sum_{k=1,3} \frac{k n_k}{2} \sqrt{\frac{k_B (T_e + T_i)}{m_{H_k^+}}}, \tag{5}$$

where k_B is the Boltzman constant, and T_e and T_i are the electron and ion temperatures, respectively. Note that detailed evaluation of the H^0 contribution in Eq. (5) would be extremely complicated, particularly if the effects of wall trapping need to be considered [14], and is far beyond the scope of the present work. For convenience, we assume that $n_{H^0} \approx n_{H^+}$ because the electron-impact Frank–Condon dissociation: $e + H_2^+ \to e + H^+ + H^0$ is the dominant process at electron temperatures 4–5 eV [11,12]. Also, it may be assumed that $T_e \gg T_i$ in Eq. (5). Using the above-mentioned densities, Γ_{total} has been calculated to be $\sim 8.3 \times 10^{16}$ H-atoms s^{-1} cm^{-2}. The incoming helium flux is estimated to be $\sim 7.8 \times 10^{14}$ He-atoms s^{-1} cm^{-2}.

3.2.2. Mixture plasma recycling experiments

Hydrogen and helium mixture plasma bombardment is conducted with the rotating drum DC-biased at −30 V and −100 V and deposited with lithium at the rate of $\sim 2 \times 10^{16}$ Li-atoms cm^{-2} s^{-1}. It should be cautioned that the actual deposition rate is slightly lower due to sputtering, which then results in lithium coatings on the wall surface. Shown in Fig. 3 is a typical example of spectroscopic data taken for H_α and He–I measured in front of the rotating drum applied with the DC bias

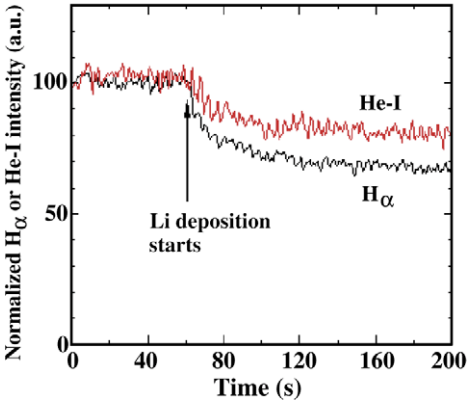

Fig. 3. Hydrogen and helium mixture plasma recycling behavior.

voltage of −100 V. From our previous work [4], these spectroscopic signals are known to be proportional to the reemitted fluxes of molecular hydrogen and hence helium as well. As soon as lithium deposition starts, both the light intensities decrease to their respective steady state levels. This suggests that hydrogen and helium are not mutually exclusive in the process of simultaneous codeposition with lithium, because they are believed to be trapped in their preferred lattice sites, as shown in Fig. 2. The observed reductions in light intensity are typically ~30% and ~20% for H_α and He–I, respectively, both relative to 100% steady state recycling. These percentage numbers correspond to the particle removal rates of $\sim 2.5 \times 10^{16}$ H-atoms s^{-1} cm^{-2} and $\sim 1.6 \times 10^{14}$ He-atoms s^{-1} cm^{-2}, and hence to the averaged atomic ratios of (H/Li) ~ 1.25 and (He/Li) ~ 0.008 in the resultant codeposits.

The somewhat larger than that is consistent with atomic ratio (H/Li) is above-mentioned the stoichoimetry of LiH, which we would attribute to the convenient assumption: $n_{H^0} \approx n_{H^+}$, having resulted in an overestimated flux to the rotating drum in VEHICLE-1, the internal surface of which is sputter-coated with lithium. In our previous work [6], H^0 along with H^+, H_2^+ and H_3^+ exhibited trapping coefficients ~0.37, orders of magnitude higher than those measured for thermal H_2, in which case one would expect that the density of H^0 be much smaller, as shown in [13]. However, again, further discussion on the hydrogenic species mix analysis is not the primary objective of the present work.

One also finds that the particle removal rates are considerably smaller than trapping coefficients, i.e. 0.85 for $H^+ \rightarrow$ Li and 0.97 for $He^+ \rightarrow$ Li at 100 eV, both calculated by the TRIM-SP code [15]. This may be a result of ion-impact desorption simultaneous with implantation, but details are unclear at this point. Although molecular dynamics calculations have yet to be executed, one predicts that trapping coefficients would noticeably be smaller when the DC bias is reduced to −30 V. Contrary to this prediction, however, spectroscopic data indicate that no significant difference has been seen between the particle removal rates obtained at −30 V and −100 V. It follows immediately from this that the particle removal rate is not quite an energy-sensitive parameter, presumably due to the continuous growth of lithium deposits. Currently, a zero-dimensional particle balance model is being developed to better interpret these observations.

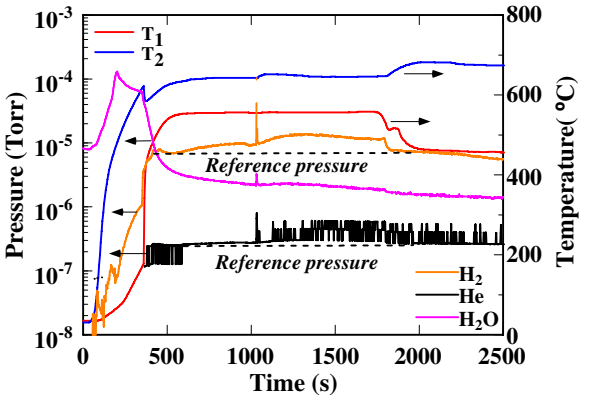

Fig. 4. Thermal desorption from bulk lithium bombarded by a H + He mixture plasma in VEHICLE-1 at the bias voltage of −100 V. The total trapping quantities of H and He evaluated, using the respective reference pressures. For the spot of temperature measurements denoted by T_1 and T_2, see Fig. 1(b) and for the details of temperature evolution, see Ref. [6]. Note that 1 Torr = 133.3 Pa.

To crosscheck these particle removal rate data, bulk lithium has also been exposed to hydrogen and helium mixture plasmas, applying the DC bias of −100 V to the sample tray shown in Fig. 1(b). Because this sample tray is not water-cooled, the ECR plasma power needs to be decreased so as to maintain lithium at around room temperature. Fortunately, the electron temperatures of mixture plasmas generated under these low-power conditions are found to be essentially the same as those measured for the rotating drum experiments, which helps avoid additional complications in the plasma species mix analysis. From the TDS data shown in Fig. 4, the time-averaged trapping rates have been evaluated to be about 5.4×10^{15} H-atoms s^{-1} cm^{-2} and 1.8×10^{14} He-atoms s^{-1} cm^{-2}, the former of which is about a factor of 5 smaller, again due to the overestimated n_{H^0}, whereas the latter of which appears to be in good agreement compared with the corresponding particle removal rate data.

4. Conclusion

In the present work, the use of MS-PFCs is proposed for particle control over wall-recycled DT fuel and helium ash in steady state fusion reactors. As the simplest form of MS-PFC, a rotating drum gettered with lithium has been exposed to steady state hydrogen and helium mixture plasmas in VEHICLE-1. Real-time H_α and He–I spectroscopic data have indicated that particles recycling is reduced noticeably, even at steady state, due to the simultaneous

hydrogen and helium codeposition with lithium, forming a multi-phase structure, i.e. Li + LiH + Li(He) where helium is trapped by lattice imperfections in vapor deposits. The particle removal rates have been estimated to be $\sim 2.5 \times 10^{16}$ H-atoms s^{-1} cm^{-2} and $\sim 1.6 \times 10^{14}$ He-atoms s^{-1} cm^{-2}. Standing samples of bulk lithium has also been bombarded with mixture plasmas under identical conditions, and post-exposure TDS data have corroborated, only qualitatively though, these particle removal rates obtained from the rotating drum setup.

Acknowledgement

Fruitful discussions on the effects of wall trapping on hydrogen plasma species composition with Professor Y. Nakashima of Tsukuba University, based on his extensive experience on the use of DEGAS code for the Gamma-10 experimental data analysis, are greatly appreciated.

References

[1] H.F. Dylla et al., J. Nucl. Mater. 162–164 (1989) 128.
[2] Y. Hirooka et al., in: Proceeding of 17th SOFE, October 6–10th, 1997, San Diego, p. 906.
[3] Y. Hirooka et al., Fusion Eng. Des. 65 (2003) 413.
[4] Y. Hirooka et al., Fusion Sci. Technol. 45 (2004) 60.
[5] Y. Hirooka et al., Fusion Sci. Technol. 47 (2005) 703.
[6] Y. Hirooka et al., J. Nucl. Mater. 337–339 (2005) 585.
[7] Y. Hirooka et al., Nucl. Fusion 46 (2006) S56–S61.
[8] E.V. Kornelsen, A.A. Van Gorkum, J. Nucl. Mater. 92 (1980) 79.
[9] S.R. Gunn, L.G. Green, J. Am. Chem. Soc. 80 (1958) 4782.
[10] E.M. Hollmann, A.Y. Pigarov, Phys. Plasmas 9 (2002) 4330.
[11] D.E. Post, R. Behrisch (Eds.), Physics of Plasma-Wall Interactions in Controlled Fusion, Plenum, New York, 1984.
[12] R.K. Janev et al., Elementary Processes in Hydrogen–Helium Plasmas, Springer-Verlag, Berlin Heidelberg, 1987.
[13] R.H. Huddlestone, S.L. Leonard, Plasma Diagnostic Techniques, Academic, New York, 1965 (Chapter. 4).
[14] S. Kobayashi et al., J. Nucl. Mater. 266–269 (1999) 566.
[15] J.P. Biersack, W. Eckstein, Appl. Phys. A34 (1984) 73.